

A Novel Vessel Segmentation Algorithm in Color Images of the Retina

Helen Ocbagabir¹, Isam Hameed¹, Sama Abdulmalik², Barkana Buket D.¹ *Member, IEEE*

¹*Department of Electrical Engineering*

²*Department of Biomedical Engineering*

University of Bridgeport

126 Park Avenue, Bridgeport CT, 06604 USA

Abstract— Diabetic retinopathy (DR) occurs in patients who have had diabetes for at least five years. Diseased small blood vessels in the back of the eye cause a leakage of protein and blood in the retina. Diagnosis of diabetic retinopathy at early stage can be done through detection of blood vessels of retina. Blood vessel segmentation is a helpful tool in the treatment of diabetic retinopathy. Many studies have been carried out in the last decade in order to get an accurate blood vessel detection and segmentation in retinal images since vascular anomalies are one of the strongest manifestations of DR. Here, we propose a ruled-based algorithm called Star Networked Pixel Tracking to decide whether a processed pixel is a part of a vessel or not. The complement of the gray scale of the green channel from the original image is used. The blood vessels are enhanced by applying a strong adaptive histogram equalization algorithm locally and globally. Morphological operations are implemented in designing a background image to generate a normalized retinal image. In order to enhance the vessels' contrast, mathematical and morphological operations are applied. Noise artifacts that look like small vessels is filtered by the proposed eight-direction network pixel tracking algorithm. The proposed method is evaluated on 20 images of well known public domain DRIVE database. We achieved an accuracy of 95.83%. This is the highest accuracy among the ruled-based methods reported for the DRIVE database.

Index Terms—fundus, retinal image, morphological operation, adaptive histogram equalization

I. INTRODUCTION

Diabetic retinopathy (DR) is a complication that occurs in the retina along with diabetes. It can lead to blindness in both middle and advance age groups [1]. The prevalence rates of retinopathy in the United States are estimated to be 40.3% for diabetic adults 40 years or older [2]. Other statistic shows that about 60% of diabetic patients for 15 years of more are affected by diabetic retinopathy. In spite of these statistics, other researches show that at least 90% of the new cases could be diminished with proper and vigilant treatment and monitoring of the eyes. Hence, it is vital for diabetic patients to have regular eye checkups [3]. Diabetic retinopathy occurs due to leakage of small vessels in retina related to prolonged period of hyperglycemia. It can be classified into two stages: Nonproliferative retinopathy and proliferative retinopathy. Nonproliferative retinopathy is the early stage of the disease which includes hemorrhage and exudates. Hemorrhage results from capillaries bleeding while exudates results from the accumulation of proteins and lipids in the retina. Proliferative retinopathy is the advance stage of the disease that new abnormal vessels, called neovascularization are grown in the retina. Thus, it can lead

to severe issues in the vision [2]. Diagnosis of diabetic retinopathy at early stage can be done through detection of blood vessels of retina. Therefore, many methods have been proposed in order to get an accurate blood vessel detection and segmentation in fundus images. Akram *et al.* used 2D Gabor wavelet to enhance the vascular pattern. They used a new multilayered thresholding technique to segment the vessels [4]. Aryanto proposed a new methodology called Max-Tree. In this method, they started with image enhancement and then applied Max-tree [5]. Selvathi and Balagopal used a supervised method to detect the vessels. Support Vector Machine (SVM) is used to classify the pixels as vessel or non-vessel. They compared their results with and without enhancement via Curvelet transform [6]. Vallabha *et al.* proposed the usage scale and orientation selective Gabor filters to detect the abnormal blood vessels [7]. Lili and Shuqian developed a novel method which depends on an adaptive local thresholding to generate binary image before extracting large vessels. They classified the tiny blood vessels with the remaining fragment by using SVM [8].

In our paper we present an original method: Star Networked Pixel Tracking Algorithm. It is used to eradicate a noise aligned in a vessel format. During the image enhancement procedure, in addition to the global adaptive histogram equalization we also applied a local enhancement to the intensity levels of the thin vessels. Moreover, morphological and mathematical operations are used to strengthen the intensity levels of the thin capillary vessels. This methodology prepares the normalized retinal image to a histogram thresholding segmentation process to create a binary image. Furthermore, logical operations are engaged to add up the locally and globally enhanced segmented binary images. Finally, artifacts obtained during the previous techniques are cleaned in the post-processing. This proposed methodology gives a high average accuracy of 95.83%. The total time required to process a single image is less than twenty five seconds, running on a PC with an Intel(R) Core(TM) i3 CPU at 2.53 GHz and 3 GB of RAM.

II. PROPOSED VESSEL SEGMENTING METHOD

This paper provides a new method for segmenting the blood vessels of the fundus captured images taken from the DRIVE public domain database. The main stages in this work can be given as: a) pre-processing; b) vessel enhancement; c) star network pixel tracking d) local enhancement; and e) vessels segmentation and post-processing.

A. Pre-processing

Red-green-blue (RGB) fundus images usually come up with low contrast and noisy background. Therefore, blood vessels, especially the thin ones, need to be enhanced to get new modified images that are more suitable for the segmentation process [9]. Our pre-processing performs global vessel enhancement and morphological methodology with image denoising.

1) Green channel extraction:

The green channel of the original image has more details than the red and blue channels. Thus, it is better to have it as a reference image for the segmentation process. Red and blue channels do not provide clear blood vessels due to the low contrast and poor dynamic range, respectively [10]. Fig.1 shows the RGB channels and how the vessels are expressed in these channels.

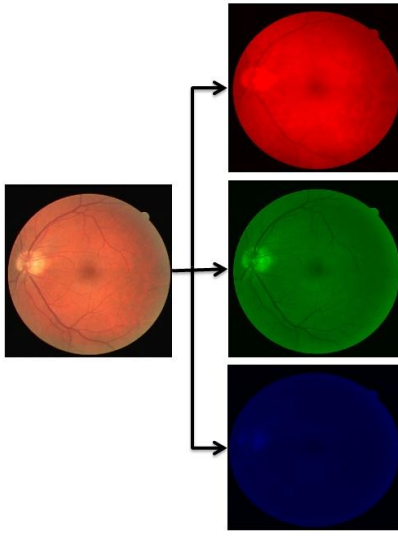


Fig. 1. Illustration of the RGB channels for a retinal image.

2) Green channel complement and adaptive histogram equalization:

In this study, adaptive histogram equalization (AHE) is used since it tends to enhance the low contrast of an image by uniformly spreading the image intensity levels. Instead of processing the entire image data, it processes small regions, individually [11]. The AHE equalizes intensity levels by making vessels, including the small ones, clearer and whiter. As a result, the image has a smoothed background. Fig.2 is showing the stages for this step that is applied on the green channel's complement to get an equalized histogram.

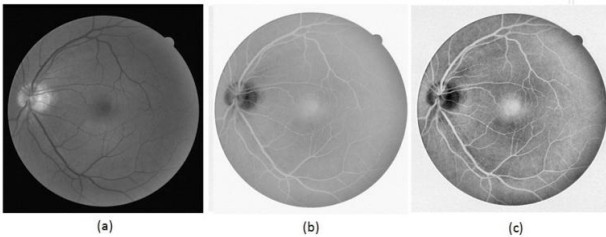


Fig. 2. Pre-processing process. (a) Original green channel. (b) Complement of the Green channel. (c) After the Adaptive histogram equalization.

3) Designing a background image to generate a normalized retinal image:

Morphological methodologies are collection of techniques used in extracting components of an image [12]. The most basic morphological operations defined are erosion and dilation. Assuming the object X and the structuring element B are represented as sets in 2D Euclidian space. Let B_x denote the translation of B so that its origin is located at x . Then the erosion of X by B is defined as the set of all points x such that B_x is included in X , that is,

$$X \ominus B = \{x: B_x \subseteq X\} \quad (1)$$

In the same way, the dilation of X by B is described as the set of all points x such that B_x hits X that is, they have a nonempty intersection

$$X \oplus B = \{x: B_x \cap X \neq \emptyset\} \quad (2)$$

Erosion is a shrinking operation, whereas dilation is an expansion operation. The erosion followed by dilation is called opening. It is defined in Eq.3 below.

$$X_B = (X \ominus B) \oplus B \quad (3)$$

Obviously, the blood vessels are suppressed by the ‘opening’ operation with a structuring element that is non-flat and ball-shaped, to create a background, I_{BK} . See Fig.3 (b). This background is used to achieve a normalized image, I_{NR} . The created background I_{BK} is subtracted from the result of the adaptive histogram equalizer, I_{ADT} , to obtain a normalized retinal image I_{NR} .

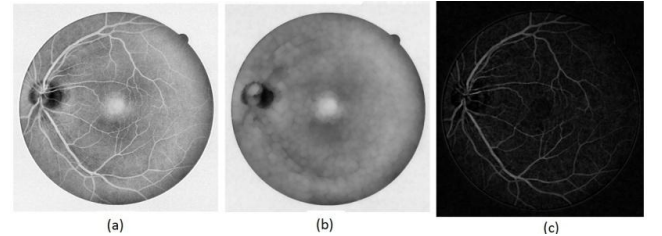


Fig. 3. Output of morphological methodology and image denoising. (a) Created Background. (b) Normalized retinal image.

Median filtering is applied to denoise occasional salt and pepper noise.

$$I_{NR}(x, y) = \text{medianfilter} \{I_{ADT}(x, y) - I_{BK}(x, y)\} \quad (4)$$

B) Vessel enhancement

During image acquisition process, contrast variations in the gray level have been noticed. In general, thick vessels show high intensity levels whereas the thin or small vessels show low intensity levels similar to the background [8]. Hence, we propose different mathematical operations to strengthen the intensity levels of the thin or small vessels with the intensity levels of background kept unchanged. This is performed by a morphological operation ‘opening’ to the normalized retinal image to create a background I_{BK} that is subtracted from I_{NR} .

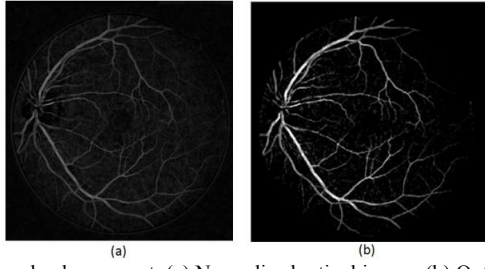


Fig. 4. Vessel enhancement. (a) Normalized retinal image. (b) Output of the mathematical operations.

The result of this subtraction I_{NR1} is opened again and the resulted background I_{BK2} is subtracted from I_{NR1} to obtain I_{NR2} . Adding I_{NR} with I_{NR2} results in a normalized retinal image I_{NR3} with improved blood vessels than that of I_{NR1} . Double background subtraction of I_{BK4} and I_{BK5} from I_{NR5} and I_{NR6} gives the image in (Fig.4) (b).

$$I_{NR1}(x, y) = I_{NR}(x, y) - I_{BK1}(x, y) \quad (5)$$

$$I_{NR2}(x, y) = I_{NR1}(x, y) - I_{BK2}(x, y) \quad (6)$$

$$I_{NR3}(x, y) = I_{NR}(x, y) + I_{NR2}(x, y) \quad (7)$$

$$I_{NR4}(x, y) = I_{NR3}(x, y) - I_{BK3}(x, y) \quad (8)$$

$$I_{NR5}(x, y) = I_{NR2}(x, y) + I_{NR4}(x, y) \quad (9)$$

$$I_{NR6}(x, y) = I_{NR5}(x, y) - I_{BK4}(x, y) \quad (10)$$

$$I_{NR7}(x, y) = I_{NR6}(x, y) - I_{BK5}(x, y) \quad (11)$$

The above mathematical operations are clarified using a flowchart shown in Fig.5.

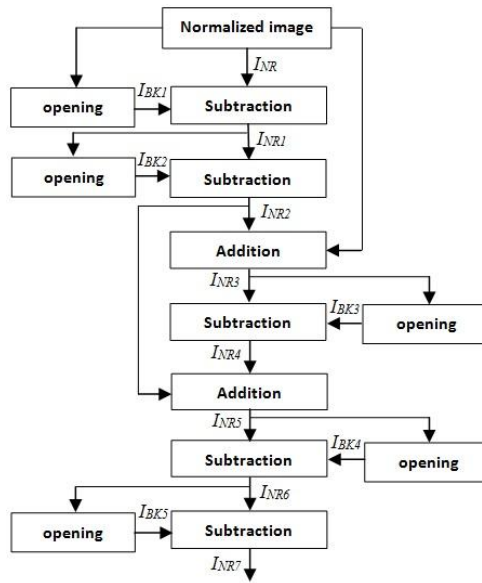


Fig. 5. Vessel strengthening flowchart

C) Star networked pixel tracking algorithm:

In order to get rid of the noise artifacts that are aligned like a small vessels, an eight direction networked pixel tracking algorithm is developed. This algorithm has the capability of distinguishing the non-vessel pixels and setting them to zero by giving an identity to the vessel pixels. In other words, the tracking process goes over the entire image pixels by comparing each pixel with its four neighboring pixels aligned in 45° to each other. This is done by applying a condition that determines whether there is a non-zero pixel in each direction or not. Once the condition finds a zero pixel, the processed pixel is considered as non-vessels. Otherwise, the last pixel in that direction will keep the same procedure one more time. This double checking will diminish the probability of noise occurrence in vessel

2) Once any direction is found to be connected, the checking process will take the last pixel in that direction as the new processed pixel.

3) The same procedure applied to the original processed pixel in Step (1) is reapplied again but in this case only seven directions are taken in consideration since we already has checked the direction from where the new processed

pixel has come.

4) When two stages (eight pixels) are checked to be connected, then the original pixel will be set as a vessel pixel. Otherwise, the pixel is set as non-vessel. Fig.7 shows the result obtained from this algorithm.

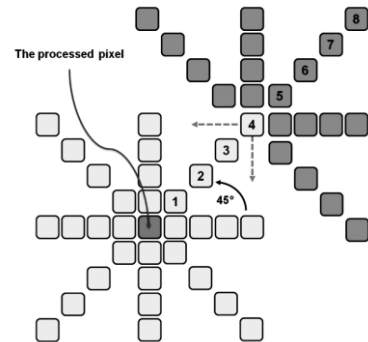


Fig. 6. Illustration of the star networked pixel tracking algorithm.

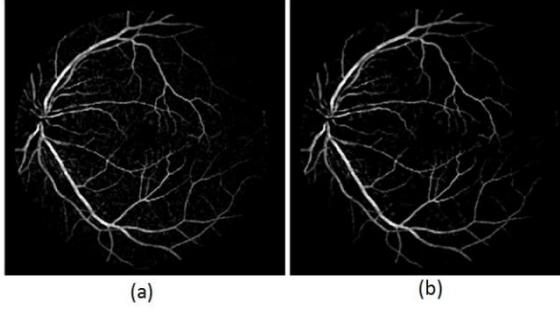


Fig. 7. The vessel enhancement and star networked algorithm (a) Output of the mathematical operations. (b) Output of the star networked pixel tracking algorithm.

D) Local Enhancement

In global enhancement, pixels are modified by a transformation function based on the gray level distribution over an entire image. Global approach is suitable for overall enhancement however it does not enhance details over small areas. Since the number of pixels in the small areas may have insignificant influence on the computation of a global transformation, these small areas do not get the desired local enhancement.

In this study, the intensity mean and standard deviation are used to identify the neighborhood of thin and small vessels. We assume that most of the thin and small vessels are to be found far from the optical disc. We used the intensity mean and standard deviation properties to locate this neighborhood. Later, we applied a linear level adjustment to the neighborhood. Linear level adjustment can be defined as:

$$P_{adjust}(m,n) = bottom + \frac{p(m,n) - L}{H - L} \times (top - bottom) \quad [12]$$

Where $p(m,n)$ is original image pixel, $P_{adjust}(m,n)$ is desired image pixel, H and L are the maximum and minimum pixel level in the original image, and top and $bottom$ are the maximum and minimum pixel level in the desired image. See Fig. 8.

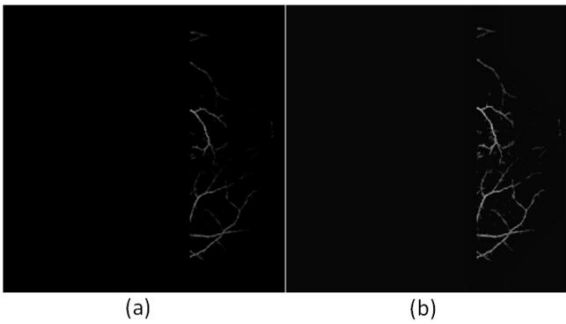


Fig. 8. Illustration of the vessel's local enhancement. (a) Before local enhancement. (b) After local enhancement.

E) Vessels Segmentation and Post-Processing

An automatic histogram thresholding is applied to the normalized and processed retinal image to extract the blood vessels from the background. Moreover, logical operation is used to combine the binary image obtained from the local

enhancement process with full normalized retinal segmented image. Finally, a post processing stage is performed in order to get rid of the small artifacts generated during segmentation. Fig.9 illustrates the binary segmented image used to combine the binary image obtained from the local enhancement process with full normalized retinal segmented image.



Fig. 9. Final segmentation.

IV. EXPERIMENTAL RESULTS

A. Performance Measures

To measure the performance of our segmentation method on fundus images of the DRIVE database, we made a comparison table that illustrates the results obtained for sensitivity (Se), specificity (Sp), positive predictive value (Ppv), negative predictive value (Npv), and accuracy (Acc) which are calculated using TP, FP, FN, and TN shown in TABLE.I [9].

TABLE I
CONTINGENCY VESSEL CLASSIFICATION [9]

| | Vessel present | Vessel absent |
|----------------------|---------------------|---------------------|
| Vessel segmented | True Positive (TP) | False Positive (FP) |
| Vessel not segmented | False Negative (FN) | True Negative (TN) |

The definitions of the taken metrics Acc , Se , Sp , Ppv , and Npv , are shown below:

$$S_e = \frac{TP}{TP + FN} \quad (12)$$

$$S_p = \frac{TN}{TN + FP} \quad (13)$$

$$P_{pv} = \frac{TP}{TP + FP} \quad (14)$$

$$N_{pv} = \frac{TN}{TN + FN} \quad (15)$$

$$Acc = \frac{TP + TN}{TP + FN + TN + FP} \quad (16)$$

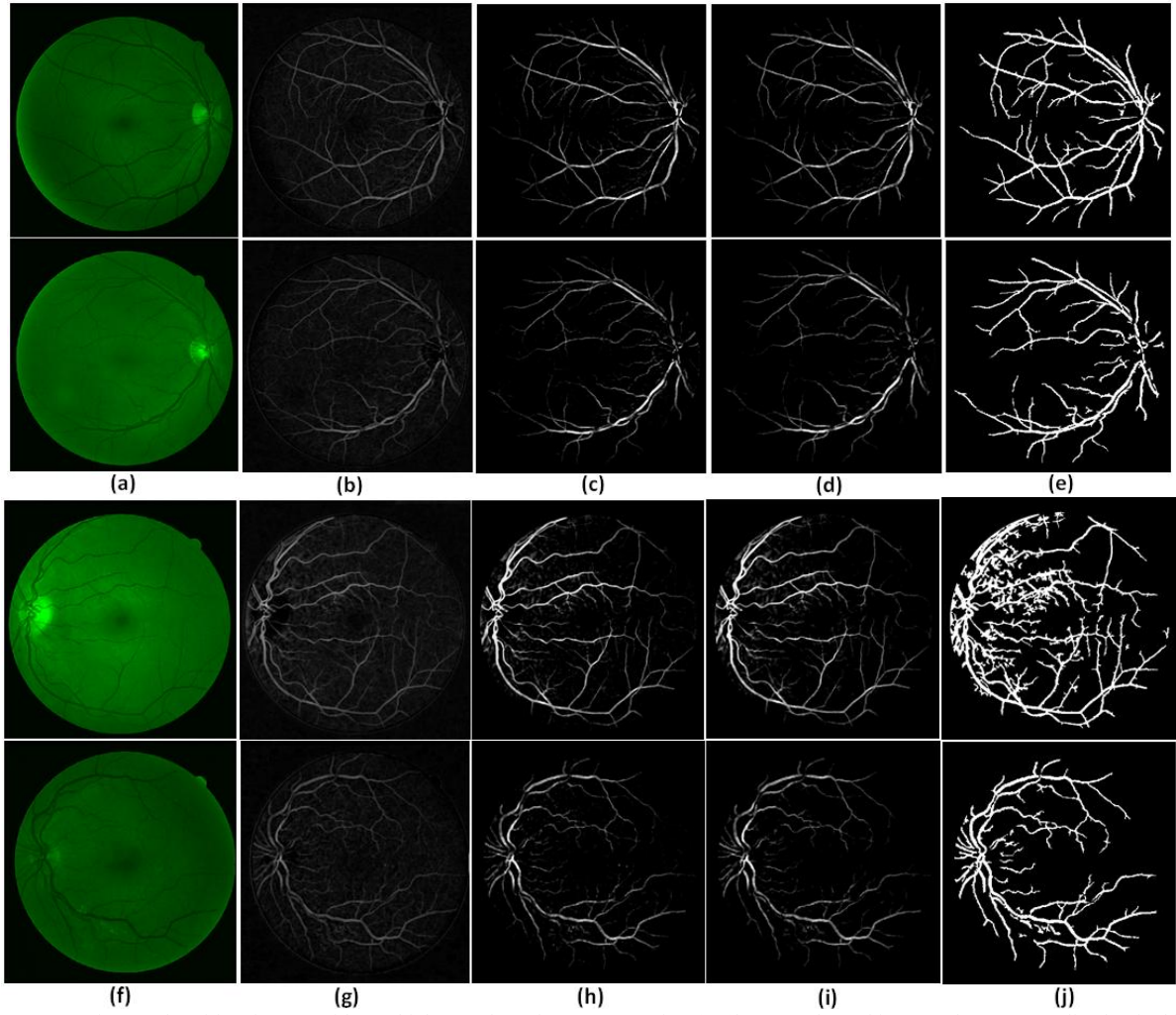


Fig. 10. Segmentation results of four images with two highest and two lowest accuracies. (a) (f) Green channel images. (b) (g) Normalized retinal images. (c) (h) Outputs of mathematical operations. (d) (i) Outputs of star networked pixel tracking. (e) (j) Final segmented images.

Where (Se) is the ratio of the vessels that are well-segmented and classified, (Sp) is the ratio of non-vessel pixels, (Ppv) represents the ratio pixels that are correctly classified as vessels, (Npv) gives the ratio of the pixels that are correctly classified as background, and Acc is the ratio of the total well classified pixels [9].

To evaluate our proposed vessel segmentation method, the DRIVE [18] database is used. The DRIVE database has been widely used by researchers to test their vessel segmentation methodologies.

The DRIVE database comprises 40 eye-fundus color images (seven of which present pathology) taken with a Canon CR5 nonmydriatic 3CCD camera with a 45 field-of-view (FOV). The database is divided into two sets: a test set and a training set. Each set contains 20 images. The test set provides the corresponding FOV masks for the images, which are circular and two manual segmentations generated by two different specialists for each image. The selection of the first observer is accepted as ground truth and used for algorithm performance evaluation in literature.

B. Comparison to Other Methods

The performance of our work is compared with previous retinal vessel segmentation works in Table III. Average accuracy was taken as measures for method performance since this measurement was performed by other authors. Table III shows the comparison with the following former

published methods: Staal *et al.* [13], Martinet *et al.* [9], Martinez-Perez *et al.* [14], Cinsdikici and Aydin [15], and Jiang and Mojon [16], Mendonca *et al.* [17].

TABLE II
PERFORMANCE RESULTS ON DRIVE DATABASE IMAGES

| Image | $Acc1$ | $Se1$ | $Sp1$ | $Ppv1$ | $Npv1$ |
|-------|---------------|---------------|---------------|---------------|---------------|
| 1 | 0.9588 | 0.8042 | 0.9739 | 0.7514 | 0.9807 |
| 2 | 0.9596 | 0.8076 | 0.9769 | 0.7998 | 0.9780 |
| 3 | 0.9523 | 0.6735 | 0.9832 | 0.8159 | 0.9645 |
| 4 | 0.9606 | 0.7175 | 0.9852 | 0.8308 | 0.9718 |
| 5 | 0.9588 | 0.6532 | 0.9904 | 0.8753 | 0.9651 |
| 6 | 0.9560 | 0.6301 | 0.9911 | 0.8845 | 0.9613 |
| 7 | 0.9541 | 0.6944 | 0.9802 | 0.7795 | 0.9696 |
| 8 | 0.9548 | 0.5919 | 0.9890 | 0.8347 | 0.9626 |
| 9 | 0.9611 | 0.6160 | 0.9915 | 0.8650 | 0.9670 |
| 10 | 0.9623 | 0.6842 | 0.9872 | 0.8277 | 0.9721 |
| 11 | 0.9505 | 0.7336 | 0.9719 | 0.7193 | 0.9738 |
| 12 | 0.9610 | 0.7143 | 0.9843 | 0.8115 | 0.9733 |
| 13 | 0.9557 | 0.6939 | 0.9841 | 0.8254 | 0.9674 |
| 14 | 0.9602 | 0.7633 | 0.9776 | 0.7496 | 0.9791 |
| 15 | 0.9534 | 0.7629 | 0.9681 | 0.6483 | 0.9815 |
| 16 | 0.9581 | 0.7254 | 0.9812 | 0.7933 | 0.9730 |
| 17 | 0.9592 | 0.6811 | 0.9848 | 0.8051 | 0.9710 |
| 18 | 0.9582 | 0.7726 | 0.9742 | 0.7204 | 0.9803 |
| 19 | 0.9672 | 0.8139 | 0.9810 | 0.7951 | 0.9831 |
| 20 | 0.9643 | 0.7287 | 0.9830 | 0.7733 | 0.9786 |
| Ave | 0.9583 | 0.7131 | 0.9824 | 0.7953 | 0.9264 |

TABLE III
PERFORMANCE RESULTS COMPARED TO OTHER METHODS ON
THE DRIVE DATABASE IN TERM OF AVERAGE ACCURACY

| Method | Accuracy |
|---------------------------|---------------|
| Staal et al.[13] | 0.9441 |
| Mendonca et al. | 0.9463 |
| Martinet al.[9] | 0.9452 |
| Martinez-Perez et al.[14] | 0.9344 |
| Cinsdikici and Aydin[15] | 0.9293 |
| Jiang and Mojon [16] | 0.8911 |
| Proposed method | 0.9583 |

III. CONCLUSIONS

We propose a retinal vessel segmentation method. Our results show that our method outperforms the other methods by achieving average 95.83% accuracy. 96.72% and 95.23% are the highest and lowest accuracies achieved by our method. The results also state that the proposed method is robust enough that it will not require user interaction in analyzing different retinal images because of its good behavior against images of different conditions.

REFERENCES

- [1] S. Ravishankar, A. Jain, A. Mittal, "Automated feature extraction for early detection of diabetic retinopathy in fundus images," *Computer Vision and Pattern Recognition, IEEE Conference on*, pp.210-217, 20-25 June 2009.
- [2] C. Hann, J. Revie, D. Hewett, G. Chase, G. Shaw, "Screening for diabetic retinopathy using computer vision and physiological markers," *Journal of Diabetes Science and Technology*, 2009 July; 3(4): 819-834, 2009.
- [3] N. Kumar, M. Pakki, "Analyzing the severity of the diabetic retinopathy and its corresponding treatment," *International Journal of Soft Computing and Engineering (IJSCE)*, Volume-2, Issue-2, May 2012.
- [4] M.U. Akram, I. Jamal, A. Tariq, J. Imtiaz, "Automated segmentation of blood vessels for detection of proliferative diabetic retinopathy," *Biomedical and Health Informatics (BHI), IEEE-EMBS International Conference on*, vol., no., pp.232-235, 5-7, 2012.
- [5] I.K.E. Purnama, K.Y.E. Aryanto, "Branches filtering approach to extract retinal blood vessels in fundus image," *Instrumentation, Communications, Information Technology, and Biomedical Engineering (ICICI-BME), International Conference on*, pp.1-5, 2009.
- [6] D. Selvathi, N. Balagopal, "Detection of retinal blood vessels using curvelet transform," *Devices, Circuits and Systems (ICDCS), International Conference on*, pp.325-329, 2012.
- [7] D. Vallabha, R. Dorairaj, K. Namuduri, H. Thompson, "Automated detection and classification of vascular abnormalities in diabetic retinopathy," *Signals, Systems and Computers, Conference Record of the Thirty-Eighth Asilomar Conference on*, vol.2, pp.1625-1629 Vol.2, Nov.2004.
- [8] L. Xu, S. Luo, S., "A novel method for blood vessel detection from retinal images," *BioMedical Engineering OnLine*, 9:14,doi:10.1186/1475-925X-9-14, 2010.
- [9] D. Marín, D., A. Aquino, M.E. Gegundez-Arias, J.M. Bravo, "A New Supervised Method for Blood Vessel Segmentation in Retinal Images by Using Gray-Level and Moment Invariants-Based Features," *IEEE Trans. Med. Imag.*, vol.30, no.1, pp.146-158, Jan.2011.
- [10] T. Walter, P. Massin, A. Erginay, R. Ordonez, C. Jeulin, and J. C. Klein, "Automatic detection of microaneurysms in color fundus images," *Med. Image Anal.*, vol. 11, pp. 555-566, 2007.
- [11] F. Hossain, M.R. Alsharif, "Image Enhancement Based on Logarithmic Transform Coefficient and Adaptive Histogram Equalization," *Convergence Information Technology, International Conference on*, pp.1439-1444, 21-23 Nov. 2007
- [12] P. Jitpakdee, P. Aimmanee, B. Uyyanonvara, "A survey on hemorrhage detection in diabetic retinopathy retinal images," *Electrical Engineering/Electronics, Computer, Telecommunications and Information Technology (ECTI-CON) Conference*, pp.1-4, 16-18 May 2012.
- [13] J. Staal, M. D. Abramoff, M. Niemeijer, M. A. Viergever, and B. v.Ginneken, "Ridge based vessel segmentation in color images

of the retina," *IEEE Trans. Med. Imag.*, vol. 23, no. 4, pp. 501-509, Apr. 2004.

- [14] M. E. Martinez-Perez, A. D. Hughes, S. A. Thom, A. A. Bharath, and K. H. Parker, "Segmentation of blood vessels from red-free and fluorescein retinal images," *Med. Image Anal.*, vol. 11, pp. 47-61, 2007.
- [15] M. G. Cinsdikici and D. Aydin, "Detection of blood vessels in ophthalmoscope images using MF/ant (matched filter/ant colony) algorithm," *Comput. Methods Programs Biomed.*, vol. 96, pp. 85-95, 2009.
- [16] X. Jiang and D. Mojon, "Adaptive local thresholding by verificationbased multithreshold probing with application to vessel detection in retinal images," *IEEE Trans. Pattern Anal. Mach. Intell.*, vol. 25, no. 1, pp. 131-137, Jan. 2003.
- [17] M. Mendonça and A. Campilho, "Segmentation of retinal blood vessels by combining the detection of centerlines and morphological reconstruction," *IEEE Trans. Med. Imag.*, vol. 25, no. 9, pp. 1200-1213, Sep. 2006.
- [18] M. Niemeijer and B. van Ginneken, 2002 [Online]. Available: <http://www.isi.uu.nl/Research/Databases/DRIVE/results.php>

Helen T Ocbagabir is a M.S. Student in the Department of Electrical Engineering at the University of Bridgeport. She received her B.S. in Electrical Engineering from University of Asmara, Eritrea in 2008. Helen worked as Graduate assistant in Eritrea Institute of Technology from a year before her graduation, 2007- 2011. Helen's interest area is in the areas of embedded systems application in Biomedical Engineering concentrating in Bio-telemetry.

Isam S. Hameed was born in Iraq, Baghdad, in 1984. He received the B.E. degree in electronic engineering from the University of Diyala, Iraq, in 2005. He is currently studying his Master degree in electrical engineering at the University of Bridgeport, CT, USA. His B.E. final project title was "Identification the system with Recursive Least Square and Improvement the Performance of the system by (PID) Controller". His Average of the four academic Bachelor years was (75.821) and he earned the first position. In 2005, he joined the Department of Electronic Engineering, University of Diyala, as a Lecturer in the laboratories up to 2009. In 2011, he was granted a scholarship from the Iraqi government to complete his Master degree in electrical engineering at the University of Bridgeport ,CT ,USA. His programming experiences is focusing on C , C + +, MATLAB, Mitsubishi and Allen Bradley PLCs ladder programming, and digital signal processor kit (DSK6713) programming using C-language. His main areas of research interest are image processing, signal processing, digital VLSI, and PLC.

Sama Abdulmalik is pursuing her masters degree in Biomedical engineering at the University of Bridgeport expected to graduate by fall 2013. She received her B.S. from King Abdulaziz University in 2007 majoring in Biochemistry with second honor.

Buket D. Barkana is an Assistant Professor in the Electrical Engineering department at the University of Bridgeport, CT. Professor Barkana is also the director of the Signal Processing Research Group (SPRG) Laboratory in the Electrical Engineering program, University of Bridgeport. Areas of her research span all aspects of speech, audio, bio- signal processing, image processing and coding. She received the B.S. in Electrical Engineering from Anadolu University, Turkey, and the M.Sc. and Ph.D. in Electrical Engineering from the Eskisehir Osmangazi University, Turkey. Dr. Barkana is a member of IEEE.